Submillisecond Unmasked Subliminal Visual Stimuli Evoke Electrical Brain Responses

Holger F. Sperdin,[1]* Lucas Spierer,[2] Robert Becker,[1] Christoph M. Michel,[1] and Theodor Landis[1]

[1]*Department of Fundamental Neurosciences, University of Geneva, Switzerland*
[2]*Neurology Unit, Department of Medicine, Faculty of Sciences, University of Fribourg, Switzerland*

Abstract: Subliminal perception is strongly associated to the processing of meaningful or emotional information and has mostly been studied using visual masking. In this study, we used high density 256-channel EEG coupled with an liquid crystal display (LCD) tachistoscope to characterize the spatio-temporal dynamics of the brain response to visual checkerboard stimuli (Experiment 1) or blank stimuli (Experiment 2) presented without a mask for 1 ms (visible), 500 μs (partially visible), and 250 μs (subliminal) by applying time-wise, assumption-free nonparametric randomization statistics on the strength and on the topography of high-density scalp-recorded electric field. Stimulus visibility was assessed in a third separate behavioral experiment. Results revealed that unmasked checkerboards presented subliminally for 250 μs evoked weak but detectable visual evoked potential (VEP) responses. When the checkerboards were replaced by blank stimuli, there was no evidence for the presence of an evoked response anymore. Furthermore, the checkerboard VEPs were modulated topographically between 243 and 296 ms post-stimulus onset as a function of stimulus duration, indicative of the engagement of distinct configuration of active brain networks. A distributed electrical source analysis localized this modulation within the right superior parietal lobule near the precuneus. These results show the presence of a brain response to submillisecond unmasked subliminal visual stimuli independently of their emotional saliency or meaningfulness and opens an avenue for new investigations of subliminal stimulation without using visual masking.

Key words: electroencephalography; visual evoked potentials; subliminal perception; tachistoscope; vision

Conflict of Interest Statement: All authors declare that the research was conducted in the absence of any financial or commercial relationships that could be construed as a potential conflict of interest.

Contract grant sponsor: Swiss National Foundation; Contract grant number: 320030-132967 (to T.L.); Contract grant sponsor: Marie Curie fellowship (to R.B.); Contract grant sponsor: European Union Seventh Framework Program (FP7/2007-2013); Contract grant number: 267171 (to R.B.)

*Correspondence to: Holger Franz Sperdin, Functional Brain Mapping Laboratory, CMU/NEUFO, 1, Rue Michel-Servet, CH-1211 Genève 11. E-mail: Holger.Sperdin@unige.ch and Theodor Landis, Department of Fundamental Neurosciences, University of Geneva, Switzerland. E-mail: Theodor.Landis@unige.ch

INTRODUCTION

From Vicary's seminal hoax with flashing the words "Drink Coca-Cola" in a movie theater [Karremans, et al., 2006] to very recent priming experiments with faces, words or, numbers, the subliminal stimuli used were generally meaningful and/or emotional. Most investigations of subliminal perception with modern electrophysiological or neuroimaging methods have used masked-priming designs to achieve subliminal presentation of meaningful or emotional information [for recent reviews, see Dehaene and Changeux, 2011; Kouider and Dehaene, 2007; Tamietto and de Gelder, 2010]. In such experimental paradigms, the subject consciously sees a stimulus, namely the mask (such as a scrambled face) while the preceding target stimulus is not consciously perceived (a face expressing an emotion). The subliminality is indirectly derived from behavioral influences of the masked stimulus. However, brain responses evoked by the mask possibly contaminate the brain responses to the target subliminal stimuli because they are superimposed in time ([see Kouider, et al., 2013], for a recent experiment using this approach).

One way to prevent the possible contamination of target-evoked brain responses by irrelevant stimuli is the presentation of the target at very short exposure. Such presentations have previously been achieved with electrical and mechanical tachistoscopes, which enables presentations of visual stimuli briefly enough to preclude conscious perception and recognition [e.g., Griffing, 1896; Karlin, 1955; Kunstwilson and Zajonc, 1980; Lancaste, et al., 1971; Merryman and Allen, 1953; Shevrin and Fritzler, 1968].

While traditional tachistoscopes have been extensively used for the behavioral exploration of subliminal perception, they were cumbersome to manipulate and not adapted for the concomitant recording of brain activity and thus, progressively abandoned in favor of computer screen solutions (CRT monitors). However, despite technological progresses, exposure times with standard computer monitors or projectors are still limited to the millisecond range with comparably low timing accuracies when brief exposure durations are used. Although visible flashes of bright light can be displayed with durations in the submillisecond range [e.g., Cobb and Dawson, 1960; Efron, 1964; Yesilyurt, et al., 2010], presenting images with very brief durations (i.e., microseconds) in a controlled and efficient manner has not yet been possible to achieve with standard PC screens and projectors [Bukhari and Kurylo, 2008; Krantz, 2000; Wiens, et al., 2004; Wiens and Öhman, 2005]. Here, we were able to reduce the exposure durations of visual stimuli briefly enough to prevent their conscious perception by developing a liquid crystal display (LCD) tachistoscope capable of displaying unmasked images for microseconds only ([Sperdin, et al., 2013]; see: http://display-corner.epfl.ch).

To our knowledge, previous literature never addressed if simple and meaningless unmasked stimuli presented subliminally for submillisecond exposure durations would nonetheless elicit reliable brain activity. To study the spatio-temporal brain dynamics underlying ultra-rapid, submillisecond unmasked subliminal visual stimulation, we applied electrical neuroimaging analyses on averaged EEG potentials evoked (VEPs) by "meaningless" full-field checkerboard visual stimuli (Experiment 1), and by white stimuli of the same luminance as the background (Experiment 2). Images were presented at three different exposure durations using a specially designed LCD tachistoscope allowing presentation durations in the submillisecond range. Stimulus visibility was assessed in a separate behavioral task (Experiment 3). The aims were to determine (i) whether visual stimuli presented without a mask and so briefly that they are not consciously seen, nevertheless elicit an evoked electroencephalographic response; (ii) whether scalp field distributions would vary depending on the duration of the exposures, and (iii) where in the brain this modulation occurs.

MATERIAL AND METHODS

Participants

Fifteen healthy subjects aged 23–39 (mean 30 years; 3 women) participated in Experiment 1. Eleven healthy volunteers aged 25–41 (mean 32 years; 1 woman) took part in Experiment 2. Seven of these subjects had participated in Experiment 1 and kindly accepted to come back for Experiment 2. All volunteers were recruited through advertisement at the Medical faculty of the University of Geneva. All reported normal hearing and sight with no previous history of neurological or psychiatric illnesses and gave their informed consent to participate in the study. Participants from Experiment 2 took part in a separate behavioral forced-choice detection task (Experiment 3) which is further detailed below. All of the subjects were right-handed [Oldfield, 1971]. Prior to the experiments, all the procedures were approved by the Ethics Committee of the Faculty of Medicine of the University of Geneva Hospital in accordance with the ethical standards proclaimed in the Declaration of Helsinki. After having pre-processed the recorded encephalographic data of Experiment 1, four participants had to be excluded due to presence of artifacts in excess.

Stimuli

In Experiment 1 (with high density EEG recordings), we presented a full-contrast black and white checkerboard (dark field = 0.13 cd/m^2; white field = 100 cd/m^2) generated with PsychoPy [Peirce, 2007]. The image was 47.8 × 26.8 cm with a pixel resolution of 1980 × 1080 (96 dpi) and had spatial frequency of three cycles per degree of

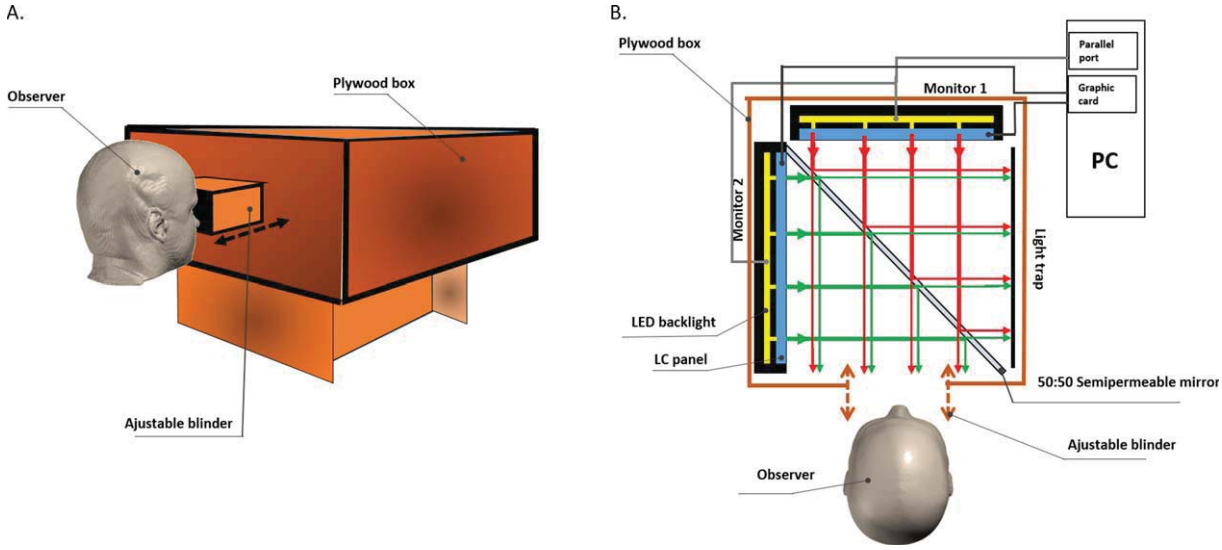

Figure 1.

A. The tachistoscope made of plywood and the observer's position. The small cut-out where the subject looks into the box has an adjustable blinder. The inside of the whole box is lined with black felt to reduce stray light. **B**. The setup consists of a 50:50 semipermeable mirror and two LCD monitors of the backlight type whose internal electronics have been modified in other to switch them instantaneously on or off (http://display-corner.epfl.ch/). [Color figure can be viewed in the online issue, which is available at wileyonlinelibrary.com.]

visual angle at 78 cm, distance at which the participants were looking at Monitor 1 (see Fig. 1A, B). In Experiment 2 (with high density EEG recordings), subjects were only presented with a white stimulus of the same luminance as the background (white field = 100 cd/m^2). Dimension and pixel resolution were identical to the checkerboard stimulus. In Experiment 3 (without EEG recordings), both stimuli were used.

Apparatus

We recently developed an LCD tachistoscope with an unprecedented precision of timing allowing the presentation of visual stimuli with exposure durations in the submillisecond range (Fig. 1A). Briefly, we used two LCD with light emitting diode (LED) backlight type monitors that are placed around a semi-permeable mirror creating the impression of seeing a single monitor only (Fig. 1B). We performed some internal modifications of the LCD electronics, to take control of the LED-backlights to almost instantly switch them on or off. A custom built adjustable eye blinder ensured that the second lateral PC screen (Monitor 2 in Fig. 1B) was not visible allowing a field of view of about 32° horizontal and 19° vertical at 78 cm distance from Monitor 1.

Prior to the experiments, we performed several measurements to test for the reliability of the tachistoscope. These measurements were done with a photodiode (Thorlabs PDA36A-EC) equipped with a lens (Pentax 50mm-F1.4) connected to a digital oscilloscope (Pico Technology PicoScope4224). Luminance was 100 cd/m^2 using a luminance photometer (Konica-Minolta LS100).

We calculated mean rise and fall times of the luminance output of about 3 μs only. Such short rise and fall times drastically reduce timing uncertainties when switching between the monitors and for the onset/duration of the stimuli. It furthers allows to produce extremely short exposure durations. Full details about the LCD tachistoscope along other measurements (e.g., LCD reaction time, LED switching characteristics, luminance output stability) can be found in Sperdin et al. ([Sperdin, et al., 2013], see also: http://display-corner.epfl.ch). Finally, we built a trigger temporizer that allowed synchronously time-locking the onset of the pulse signal of the screen switch with the EEG amplifier.

Presentation and Timing

Presentation and timing of stimuli were controlled by a custom written script using Psychophysics Toolbox extensions [Brainard, 1997] in Matlab environment (Natick, MA, http://www.matlab.com). The LED backlight was controlled through the parallel port of the experimental PC. We used a function called parPulse that accesses the parallel port directly on the hardware register level to generate short output pulses (see http://display-corner.epfl.ch/

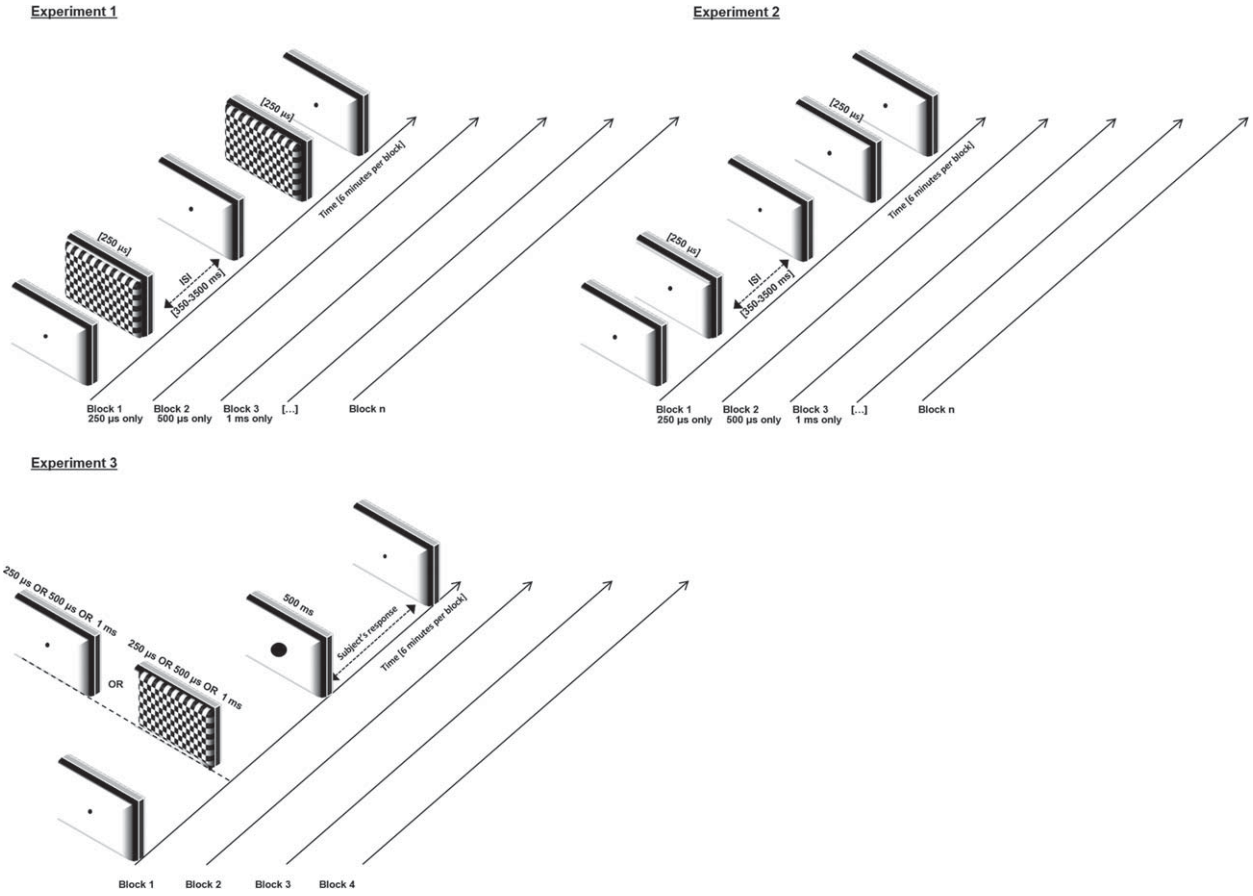

Figure 2.

Experimental design for Experiments 1, 2, and 3. Experiment 2 was identical in all respect to Experiment 1 except for the stimulus that was used. Here, the checkerboard stimulus was replaced by a stimulus with the same luminance as the background of Monitor 1. Each session started with the fastest exposure duration (250 µs followed by 500 µs and 1 ms). Each sweep had a randomized ISI varying between 350 and 3500 ms. In Experiment 3, subject had to maintain their gaze on a small centrally presented black dot. A stimulus (the checkerboard or the white screen) was then flashed for one of the three exposure durations (250 µs or 500 µs or 1 ms). After the flash, the small dot changed its size for 500 ms and at that point, subjects had to indicate whether they had seen something before the change of size or not.

index.php/ParPulse). Briefly, parPulse uses the high-precision timer for timing the pulse width and raises momentarily the central processing unit priority to its maximum. Synchronicity and duration of the chosen exposures (1 ms; 500 µs; 250 µs) was verified with an analogue oscilloscope (Hameg HM400).

Procedure and Task

All experiments were conducted in a dimly lit soundproof Faraday cage. In Experiment 1, subjects were informed that they would be presented with a stimulus, which would briefly be flashed from time to time. They were subsequently told that they had to sit quietly with their head placed on a chin-rest, and maintain their eyes on a black fixation dot presented centrally on a white background. The experimental recordings always started with the fastest exposure duration (block one, only 250 µs trials). Then, a second block was recorded that only comprised trials with the intermediate exposure duration (i.e., 500 µs). The third block only comprised the 1 ms level of the tested variable. We then run five additional blocks to accumulate sufficient trials for subsequent analysis. Each block had an approximate duration of 6 min (see Fig. 2, Experiment 1). No response was required as we wanted to record the purest EEG signal not contaminated by motor responses. Exposure durations were chosen to cover a range of duration resulting in the stimulation being either completely unperceived (250 µs) or detected as a faint

flicker (1 ms). On average, all participants were exposed with at least 150 trials, 400 trials, and 800 trials for the 1ms, 500 μs, and 250 μs exposure durations, respectively. To minimize anticipation and expectation, we did not instruct participants with regard to what type of nor how many stimuli would be presented. The inter-stimulus interval was randomly determined between 350 and 3500 ms to avoid anticipation.

Experiment 2 was identical to Experiment 1 in all respects, with the exception of the visual stimulus that was used (see Fig. 2, Experiment 2). We simply replaced the checkerboard stimulus with a white stimulus of the same luminance as the background so that the recording setting remained the same but no actual change was apparent on the screen. This was done to control for any possible artifacts inherent to the stimulation apparatus.

Assessment of Stimulus Visibility

We assessed stimulus visibility using both subjective and objective measures. During the passive presentations (Experiments 1 and 2), we asked at the end of each block what the subjects had perceived. Participants of Experiment 2 also underwent a separate forced-choice detection task without EEG recording. The subjects were instructed to pay attention and to maintain their gaze on a small dot presented centrally on a white background. They were told that stimuli would be briefly flashed from time to time. To cue them as to when to respond, we told them that the fixation dot would briefly change its size for 500 ms every 2 to 3 sec and return to its normal size. At that point they had to respond as to whether something had been flashed before the change of size or not. The stimuli were flashed at random intervals between 1000 and 1500 ms before the fixation changed its size. We instructed them to press on the right button of the response pad with their right index finger whenever they thought they had seen "something" or the left button with their left index finger if they saw "nothing." We insisted that they had to press the button "I saw something" whenever they had the faintest feeling of having seen something. Hand assignment was counterbalanced between blocks. The same stimuli and exposure durations were used as for the passive EEG recordings of Experiments 1 and 2. The subjects completed 4 blocks of 90 trials (360 trials altogether, divided between the six stimulation conditions (2 stimuli (white\checkerboard) $\times$ 3 durations (250 μs\500 μs\1 ms), randomly intermixed; see Fig. 2, Experiment 3).

Along with detection rates, participants' performance was analyzed according to signal detection theory [Green and Swets, 1988]. Sensitivity (d') was calculated according to the following formula: $d' = z\,(\mathrm{H}) - z\,(\mathrm{FA})$; where z (H) and z (FA) represent the transformation of the hit and false-alarm rates into z-scores [Macmillan and Creelman, 2005]. Hits were the checkerboard stimuli correctly detected (i.e., pressing the button for "I saw something"). False alarms were the white stimuli erroneously detected (i.e., pressing the button "I saw something"; see [Naccache and Dehaene, 2001] for a similar approach).

EEG Acquisition and Preprocessing

The EEG was acquired using a Hydrocel Geodesic Sensor Net (HCGSN, Electrical Geodesics, USA) with 256 scalp electrodes at a sampling frequency of 1000 Hz. Online recording was band-pass filtered at 0–100 Hz (vertex as reference) and impedances were maintained below 30 kΩ. After three recording blocks, impedances were rechecked as to maintain them below this threshold. Data pre-processing were done using Cartool Software ([Brunet et al., 2011]; http://sites.google.com/site/fbmlab/cartool).

The raw data were offline recalculated against the average reference and filtered using a 0.58–40 Hz Butterworth band pass filters. Using first an automatic rejection of trials showing amplitudes values exceeding ± 80 μV, single trials epochs from -75 to 400 ms post-stimulus onset (i.e., 75 data points before and 400 data points after stimulus onset) were selected for analysis and all sweeps were manually inspected one by one to exclude trials with transient noise subsequent to blinks, eye movements, or other sources. For subsequent analysis and prior to group averaging, the montage was down sampled to a 204-channel electrode array to exclude electrodes at the cheek and the neck. For each participant and when necessary, channels exhibiting substantial noise were interpolated using spherical spline interpolation [Perrin et al., 1987]. Finally, a baseline correction was applied over the prestimulus onset period.

EEG ANALYSIS

General Analyses Strategy

We first analyzed the event-related potential (ERP) recordings using global data-driven randomization statistics to find evidence of the presence of a signal (i.e., an evoked response) as opposed to noise for the three exposure durations, and for both experiments separately. Next, the difference between the brain responses to the three exposure durations was analyzed by applying time-wise statistics on all electrodes, on the strength and on the topography of the scalp-recorded electric field [Koenig et al., 2011; Koenig and Melie-Garcia, 2010; Koenig et al., 2013; Murray et al., 2008; Nichols and Holmes, 2002] according to a one-way ANOVA with exposure duration (250 μs, 500 μs, and 1 ms) as within-subjects factor. As a final step, we estimated the source of our effects by applying the local autoregressive average (LAURA) regularization approach.

Topographic Consistency Test Analysis

The topographic consistency test (TCT) aims at identifying in the EEG data the presence of a signal (i.e., an ERP)

that is significantly different from noise [Koenig et al., 2011; Koenig and Melie-Garcia, 2010]. This issue is critical in this study because one of our main questions was to determine if the brain responds to subliminal meaningless stimuli. TCT assumes that if there is a brain response functionally related to repeated presentation of stimuli (i.e., if the brain responses to the presented stimuli were not only noise), this brain response would then be similar across participants. The test for between-participant consistency is based on measures of the Global Field Power (GFP) [Lehmann and Skrandies, 1980]. The GFP is a global field strength measure that depends on the amount of signal and the variance of the experimental data across channels. It equals the spatial standard deviation of the electric field measured at the scalp and is calculated as the square root of the sum of all squared potentials divided by the number of electrodes [Lehmann and Skrandies, 1980; Murray et al., 2008]. The rationale behind the TCT is that the more the topographies are consistent across the individual ERPs, the higher is the GFP of the group-averaged ERP as compared to the average of the individual GFP. Thus, the comparison between the GFP of the group-averaged ERP and the average of the GFP of the individual ERP can be used as the effect size of the topographic consistency. On this basis, we estimated the topographic consistency as follows: for each participant and exposure durations, the measured potentials across electrodes in each individual ERP map were permuted 5000 times to generate a randomized data set corresponding to a situation where the individual ERPs are only noise (i.e., the topographic information is destroyed while preserving the GFP). Then, the probability that the measured ERPs are only noise equals the percentage of the 5000 randomizations in which the GFP in the group mean of the actual ERP is higher than the GFP of the group mean of the shuffled data. This procedure was performed for the grand means VEPs of the three exposure durations (1 ms; 500 μs; 250 μs) when using a simple checkerboard (Experiment 1) and a white stimulus (Experiment 2) using the RAGU software [Koenig et al., 2011]. Only the effects meeting or exceeding the $P < 0.001$ criterion for at least 25 consecutive data points (25 ms) were considered as reliable [Guthrie and Buchwald, 1991].

Voltage Waveform Analysis

We contrasted VEPs between the three exposure durations (1 ms; 500 μs; 250 μs) at each scalp electrodes using a time-wise, electrode-wise ANOVA with exposure duration as within-subjects factor. Only the effects meeting or exceeding the $P < 0.001$ criterion for at least 25 consecutive data points (25 ms) were considered as reliable [Guthrie and Buchwald, 1991]. In addition to these single-channel analysis, reference-independent spatiotemporal methods based on global measures of the electric fields were applied [Michel, 2009; Michel and Murray, 2012; Michel et al., 2004; Murray et al., 2008].

GFP Analysis

Differences in GFP as a function of time post-stimulus onset between exposure durations were analyzed using a simple one-way ANOVA with again the exposure duration (1 ms; 500 μs; 250 μs) as within-subjects factor and randomization statistics based on the procedure described for the TCT: GFP at each time point was compared with an empirical distribution derived from a bootstrapping procedure (5000 permutations per data point) based on randomly reassigning each participants data to one of the three durations [Koenig et al., 2011; Koenig and Melie-Garcia, 2010]. Only effects meeting or exceeding the $P < 0.001$ criterion were considered as reliable. To correct for temporal correlations, we applied a 25 time frames criterion for the persistence of sustained differential effects [Guthrie and Buchwald, 1991].

Global Map Dissimilarity Analysis

To assess the presence of topographic modulations across each level of the variable duration, we also applied randomization statistics to the global dissimilarity index (DISS) which represents a single global measure of a difference between two given electric field maps [Lehmann and Skrandies, 1980; Murray et al., 2008]. DISS is a global reference independent measure insensitive to amplitude modulations across experimental conditions and is mathematically equivalent to the root mean square of the difference between strength-normalized vectors. As for the GFP analysis, we analyzed DISS values as a function of time post-stimulus onset according to the one-way ANOVA with duration (1 ms; 500 μs; 250 μs) as within-subjects factor using RAGU software [Koenig et al., 2011; Koenig and Melie-Garcia, 2010]. The measure of effect size is here called generalized dissimilarity [Koenig and Melie-Garcia, 2009]. As the design contains three conditions, the test statistics used is based on residual maps representing the variance of the condition wise maps that are obtained by subtracting the grand-mean map across all conditions. First, the algorithm calculates the grand mean across all conditions. This grand mean map is then subtracted from the VEPs of all subjects and all conditions to obtain the individual residual maps. Subsequently, the grand means of the residual maps for each condition are calculated. After these steps, the generalized dissimilarity based on the condition is computed. The residual maps across conditions in each subject are randomly shuffled and the condition-wise grand means of the residual maps after randomization are recomputed 5000 times. Then, the probability that the maps are similar equals the percentage of the 5000 randomization runs in which the effect size obtained after randomization is equal to or larger than the effect size obtained in the observed data. Only effects meeting or exceeding the $P < 0.001$ criterion were considered as reliable and temporal auto-correlation was corrected through the application of a >25 successive temporal data-point criterion [Guthrie and Buchwald, 1991].

Source Estimations

As a final step, we estimated the source of our effects by applying a distributed linear inverse solution based on LAURA regularization [Grave de Peralta Menendez et al., 2001; Grave de Peralta Menendez et al., 2004]. The lead field was calculated using a standard array with the 204 electrode positions, the average Montreal Neurological Institute (MNI) brain template in a grey matter constrained simplified realistic head with 5018 equally distributed solution points [Brunet et al., 2011]. Source estimations were then calculated over the time windows determined through the above DISS analysis. Before doing so, the signal-to-noise ratio of single-subject data was increased by averaging the data over the significant time windows to generate a single data point for each subject and level of the variable exposure duration. Statistical analyses were then performed with one-way repeated measures ANOVA with the independent variable duration (250 μs, 500 μs, and 1 ms) as within-subjects factor using the STEN toolbox (http://www.unil.ch/fenl/home/menuinst/about-the-line/software–analysis-tools.html). To partially correct for multiple testing, we applied a significance threshold of $P < 0.001$, with a spatial extent criterion of 12 contiguous nodes. Brodmann areas (BA) and coordinates based on the system of Talairach and Tournoux [1988] are reported. [Talairach and Tournoux, 1988].

RESULTS

Behavioral Results

In Experiments 1 and 2, we asked at the end of each block what the subjects had perceived. For the first experiment, participants reported seeing slight flickers from time to time mostly in the 1 ms condition. For Experiment 2, participants indicated that the screen remained white (no change) throughout the recording session. Objective measures of stimulus visibility were obtained in the behavioral forced-choice detection task (Experiment 3).

The mean percentage of correct hit rate for the checkerboard stimulus equaled 2.3% ± 1.6 (mean ± SEM), for the 250 μs duration, 33.2% ± 8.8 (mean ± SEM) for the 500 μs duration and 81.9% ± 6.05 (mean ± SEM) for 1 ms duration. Detection rates were submitted to a repeated measures ANOVA using duration as the within-subjects factor. There was a significant main effect of factor duration ($F_{(2,9)} = 84.064$, $P < 0.0001$; $\eta_p^2 = 0.949$). Post hoc contrasts showed that detection rates was lower in the 250 μs condition as opposed to the 500 μs ($P < 0.003$) and the 1 ms conditions ($P < 0.0001$). This indicates that participants could not detect stimuli in the 250 μs, where at chance for the 500 μs but more consistently detected the visual stimuli as faint flickers in the 1 ms condition. This result is consistent with the verbal reports obtained for the passive experiments. The mean percentage of correct rejection rate for the white background stimulus equaled 98.1% ± 0.5 (mean ± SEM), for the 250 μs duration, 98.2% ± 0.6 (mean ± SEM) for the 500 μs duration and 95% ± 1.6 (mean ± SEM) for 1 ms duration. Correct rejection rates were likewise submitted to a repeated measures ANOVA using exposure duration as within-subjects factor. As expected correct rejection rates did not differ significantly across exposure durations ($P > 0.386$). This is consistent with the verbal reports that the screen was perceived as remaining white throughout the recording sessions.

We then analyzed detection sensitivity (d'). For the 250 μs exposure condition, individual d' values ranged from −1.44 to +0.46 (mean +0.33, ± SEM 0.18). This distribution did not differ significantly from a zero-centered Gaussian (Z-test, $P = 0.078$). This indicates that the checkerboards stimuli were subliminal for the 250 μs condition. Detection sensitivity increased in the 500 μs condition with d' values ranging from +0.18 to +2.7 (mean +1.66, ± SEM 0.26). This distribution differed significantly from a zero-centered Gaussian (Z-test, $P < 0.0001$). Finally, best performances were found in the 1 ms condition where d' values ranged +0.22 to 4.76 (mean +2.83, ± SEM 0.34). This distribution differed significantly from a zero-centered Gaussian (Z-test, $P < 0.0001$). Sensitivity in stimulus detection was further submitted to a 1 × 3 within-subjects ANOVA, using duration as factor. This analysis revealed a main effect of duration ($F_{(2,9)} = 63.129$, $P < 0.001$; $\eta_p^2 = 0.933$). As for the detection rates, follow-up contrasts indicated that d' values were significantly lower for 250 μs condition than for either 500 μs condition ($P < 0.001$) or 1 ms condition ($P < 0.001$); the latter two of which did significantly differ ($P < 0.003$).

EEG Results

Figure 3A shows butterfly plots of the group-average visual evoked response to the three exposure durations (in black, red, and green for 1 ms, 500 μs, and 250 μs, respectively) obtained in Experiment 1 (left butterfly) and Experiment 2 (right butterfly). As can be seen by visually inspecting the superimposed waveforms obtained in Experiment 1, the evoked responses were strongest in amplitude for the 1ms, followed by the 500 μs, whereas the 250 μs evoked the lowest amplitudes. In contrast, the visual inspection of the VEPs obtained in Experiment 2 indicates no particular amplitude modulations (i.e., no evoked response is suggested). Figure 3B shows eight exemplar individual electrodes to further identify the presence of components in the VEPs obtained in Experiment 1 (left graph) and Experiment 2 (right graph). As can be seen by visually inspecting the single electrodes waveforms, components are present in the checkerboard condition whereas totally absent when the blank screen was used.

Topographic Consistency Test

As a first step of analysis, we applied a TCT to the VEPs for the three exposure durations of Experiment 1

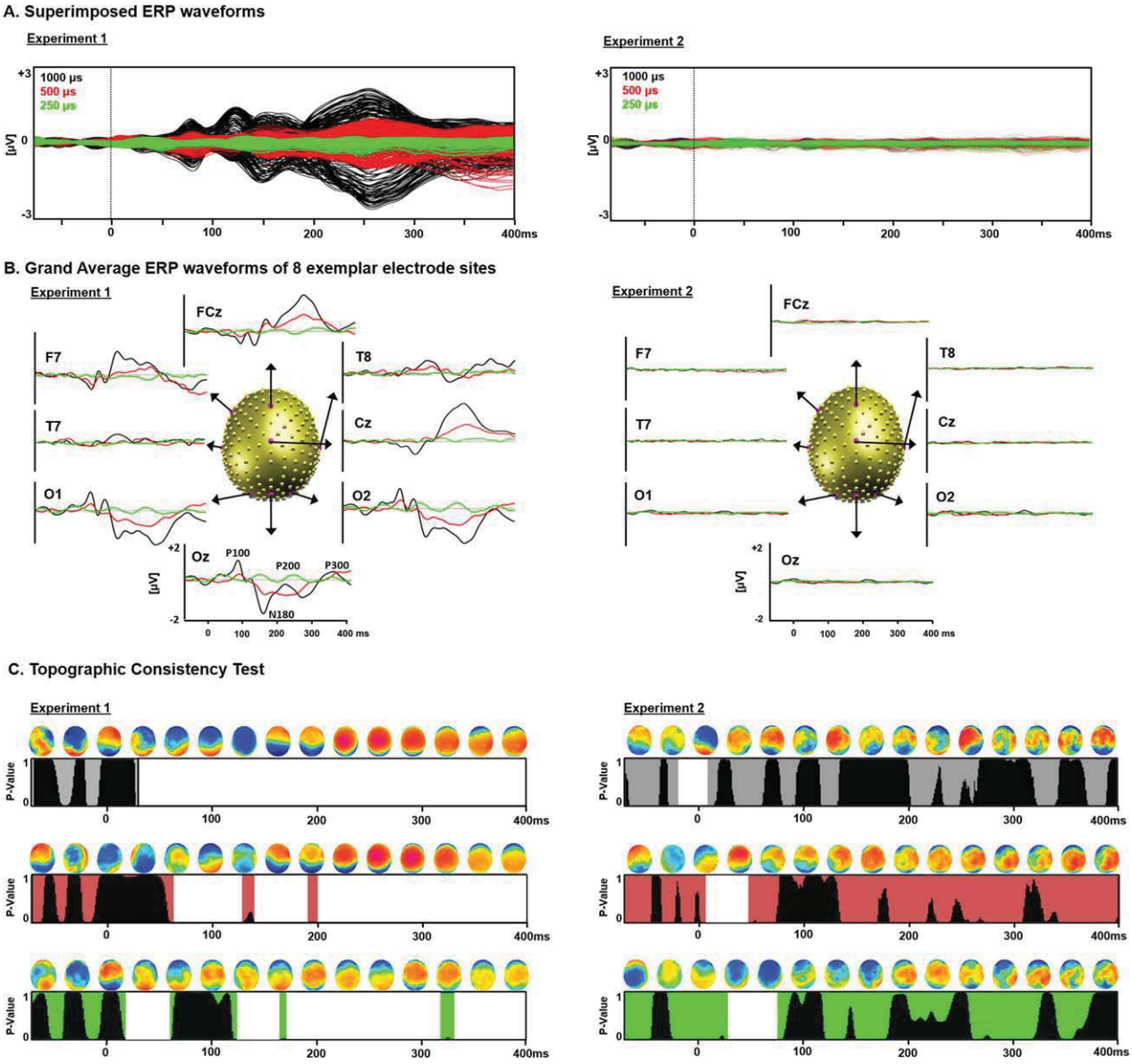

Figure 3.

A. Superimposed ERP waveforms in response to 1 ms (black), 500 µs (red), and 250 µs (green) obtained in Experiment 1 (left graph) and Experiment 2 (right graph). The *x*-axis displays the time from −75 to 400 ms post-stimulus onset and the *y*-axis amplitude in microvolt. **B**. Grand Average ERP waveforms of eight exemplar electrode sites (F7, FCz, T7, T8, Cz, O1, Oz, O2) obtained in Experiment 1 (left) and Experiment 2 (right).**C**. Time-wise Topographic Consistency Test (TCT) and corresponding maps of the grand mean VEPs in response to the exposure durations (1 ms [black], 500 µs [red], 250 µs [green]) in Experiment 1 (left) and Experiment (2). The *x*-axis displays the time from −75 to 400 ms post-stimulus onset. The left vertical *y*-axis indicates the *P*-value resulting from the tests. Colored-out regions indicate inconsistent topographies whereas periods of consistent topographies are displayed in white.

when the checkerboard was used (left graph) and of Experiment 2 when the blank screen was used (right graph). This was done to delineate the subsequent statistical analysis to time periods where positive evidences of a regular relation between stimuli presentations and activations of brain electric sources were found. For Experiment 1, the test revealed the presence of sustained and significant ($P < 0.001$) periods of stable topographies across

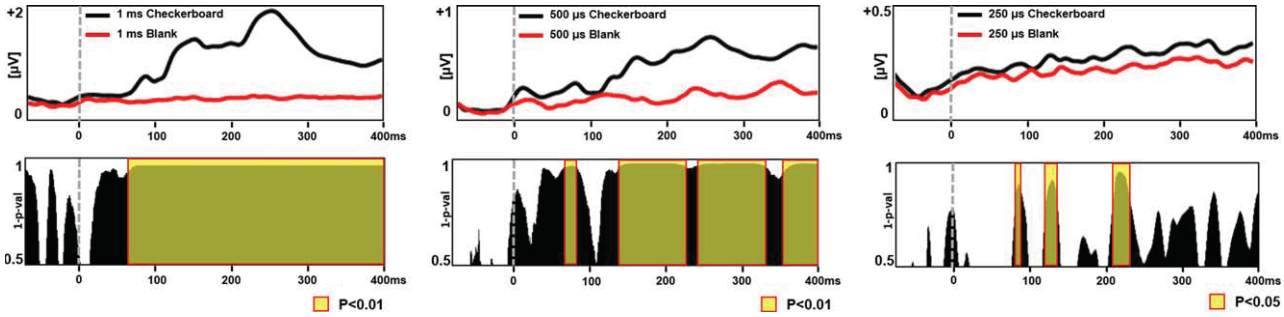

Figure 4.

Mean GFP waveforms in response to the checkerboard stimuli (black line) and to the blank stimuli (red line) for the three exposure durations (1 ms [left], 500 µs [middle], and 250 µs [right] panels). Periods of significant differences in response strength are marked in yellow. Note the different scaling on the *Y* vertical axis. [Color figure can be viewed in the online issue, which is available at wileyonlinelibrary.com.]

subjects and exposure durations (in white). Specifically, the 1 ms condition revealed periods of consistency from 24 to 400 ms post-stimulus onset with no period of inconsistent topography. The 500 µs condition revealed periods of consistent topographies between 56 and 400 ms post-stimulus onset, with brief periods of inconsistent topographies between 129 and 137 and 193 and 196 ms. Finally, the shortest exposure duration of 250 µs also revealed periods of consistencies between 16 and 400 ms, with periods of inconsistencies between 60 and 120 ms, 165 and 171, and 318 and 326 ms. In Experiment 2, the TCT only revealed early short-lived periods of topographic consistency between 24 and 76 ms in the 250 µs condition, between 5 and 46 ms in the 500 µs condition and between −35 to 8 ms in the 1 ms condition.

Having first identified the time periods of consistent topographies, we then aimed at identifying when the strength of brain responses to the checkerboards differed as compared to when a white blank screen was presented. To do so, we contrasted the mean GFPs between the checkerboards and the blank screen conditions for all three exposure duration separately. Mean GFP waveforms are displayed in Figure 4. Visual inspection of these waveforms suggests that stronger brain responses were present in response to checkerboard stimuli as opposed to blank stimuli for all three exposure durations. This observation was statistically tested via time-frame wise nonparametric randomization tests. There was evidence for changes in response strength as a function of stimulus in the 1 ms condition over the 65–400 ms post-stimulus onset ($P < 0.01$; unpaired; one-tailed). In the 500 µs condition, there were stronger brain responses to checkerboards over the 74–84 ms and 141–228 ms, 239–333 ms and 363–400 ms post-stimulus onset periods ($P < 0.01$; unpaired; one-tailed). Finally, in the 250 µs condition, the GFP was stronger in response to the checkerboard stimuli between 83 and 89 ms, 124 and 134 ms, and 211 and 229 ms post-stimulus onset ($P < 0.05$, unpaired; one-tailed). This indicates that the checkerboard elicited in all cases stronger brain responses as compared to when the blank screen was used.

As Experiment 2 was only used to rule out that artifacts of the apparatus setting could explain our effects, we focus the remaining analyses on the data of Experiment 1 in which a checkerboard was used.

ERP Waveform Modulations

Figure 5A displays the result of a time-wise, electrode-wise repeated measures ANOVA on the VEPs of Experiment 1. The main effect is displayed as an intensity plot with *x*-axis representing time, *y*-axis the electrodes positions, and *z*-axis the P-values of the ANOVA. The main effect manifested principally over 100–150 ms over the right and occipital electrodes and between 200 and 300 ms over the frontal, right, left and occipital electrodes.

Global Field Power

As can be seen, the strongest fields were measured for 1 ms exposure duration, followed by the 500 µs and 250 µs (Fig. 5B). The timeframe wise one-way repeated measures ANOVA with exposure duration (1 ms; 500 µs; 250 µs) as within-subjects factor on GFP revealed a significant ($P < 0.001$) main effect between 86 and 220 ms and 224 and 370 ms post-stimulus onset periods (Fig. 5C).

Global Map Dissimilarity Analysis

The timeframe wise one-way repeated measures ANOVA with exposure duration as within-subjects factor of global DISS revealed a significant ($P < 0.001$) main effect over the 243–296 ms post-stimulus onset period, indicating different map topographies and thus suggesting the engagement of

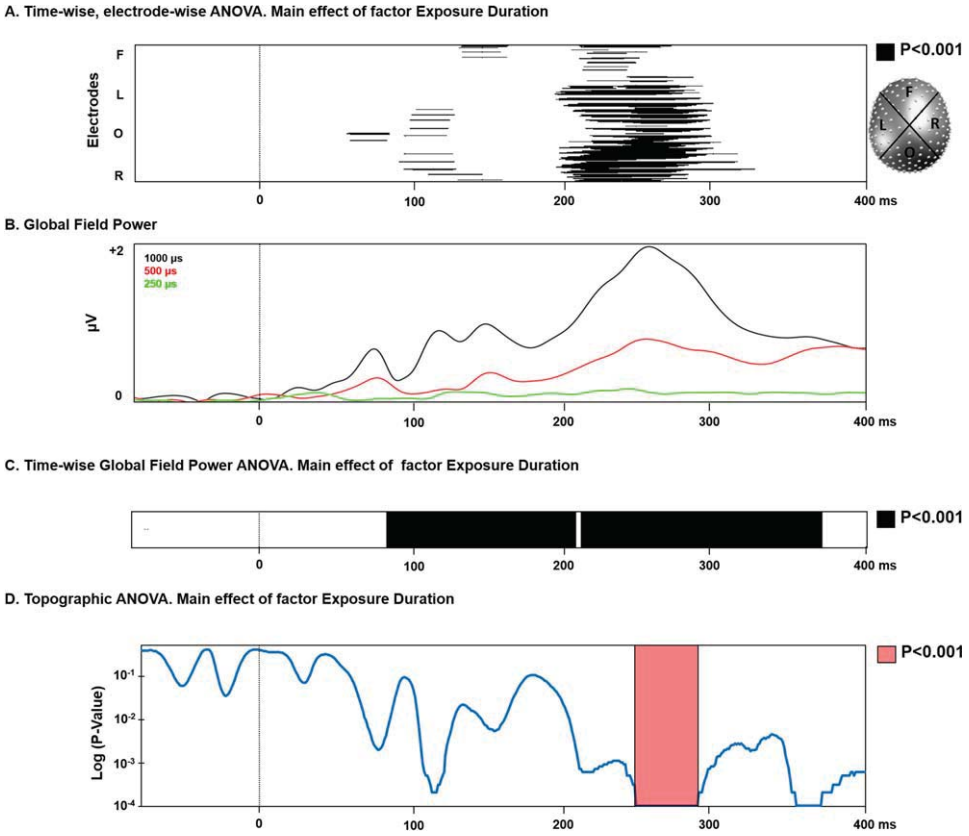

Figure 5.

A. Time-wise, electrode-wise repeated measures ANOVA: main effect of factor exposure duration. The *x*-axis represents time from −75 to 400 ms post stimulus onset, the *y*-axis the electrodes position ([F], frontal, [L] left, [O], Occipital, [R], right) and *z*-axis the *P*-values of the main effect ($P < 0.001$ at least 25 consecutive milliseconds). **B.** Global field power waveforms. The *x*-axis displays the time from −75 to 400 ms post-stimulus onset with *y*-axis indicating the GFP value in microvolt in response to 1 ms (black), 500 µs (red), and 250 µs (green). **C.** Time-wise global field power ANOVA with main effect of factor exposure duration displayed in black ($P < 0.001$ at least 25 consecutive milliseconds). **D.** Topographic ANOVA: main effect of factor exposure duration at 243–296 ms post-stimulus (in red) indicative of the engagement of distinct configurations of active brain networks ($P < 0.001$ for at least 25 consecutive milliseconds). The *x*-axis displays the time from −75 to 400 ms post-stimulus onset with *y*-axis indicating the decadic logarithm of the *P*-values resulting from the tests. [Color figure can be viewed in the online issue, which is available at wileyonlinelibrary.com.]

different intracranial source generators over this specific time period across the three exposure durations (Fig. 5D).

Source Estimations

We calculated distributed source estimations over the 243–296 ms post-stimulus period, that is, when the DISS (i.e., topographic) analysis showed the significant main effect of factor duration. First, we separately averaged the VEPs for each participant and each level of the variable exposure duration between 243 and 296 ms post-stimulus to generate one single data point per subject and experimental level of the variable. Source estimations were then calculated and the scalar value of each solution point (i.e., the current density) was submitted to repeated measures ANOVA with duration (1 ms; 500 µs; 250 µs) as within-subjects factor with a minimum cluster of 12 nodes. The main effect ($P < 0.001$, >12 contiguous nodes) revealed a modulation principally within the right superior parietal lobule (BA 7; 29, −62, 56) comprising the precuneus and a small portion of the cuneus within the occipital lobe (BA 19; 8, −81, 35; Fig. 6).

DISCUSSION

In this study, we showed that: (1) visual stimuli without emotional saliency or meaningfulness presented without a mask so shortly (submillisecond range) that not even the

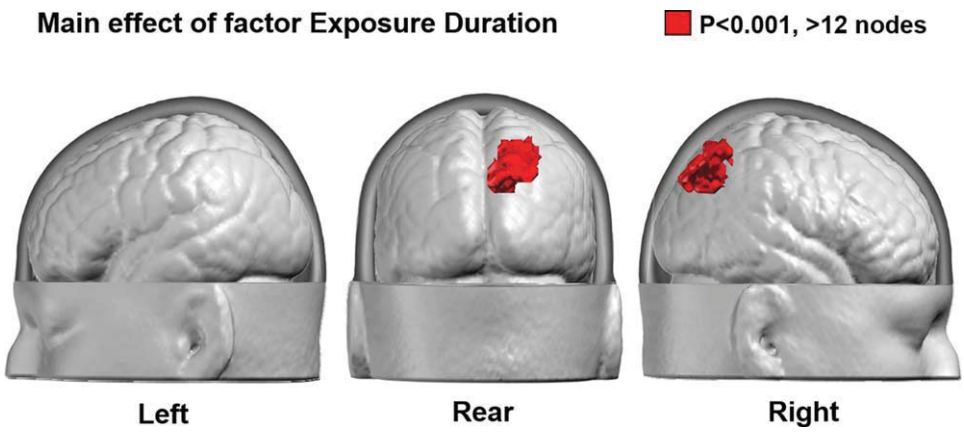

Figure 6.

Electrical source estimation over the 243–296 ms period showing significant topographic modulation (left, rear, and right sided view, respectively) displayed on the MNI template brain (main effect of factor exposure duration, $P < 0.001$, >12 nodes). [Color figure can be viewed in the online issue, which is available at wileyonlinelibrary.com.]

slightest flicker of a uniformly white screen can be seen nor be objectively detected, nevertheless produced a consistent, long lasting EEG response that can be tracked; (2) the topography of the EEG response is modulated by the duration of the exposures (1 ms; 500 μs; 250 μs), and (3) the modulation locates in the right parietal region.

The possibility that a subliminal stimulus may be responded to by the brain and influence subjects' subsequent behavior is a long-standing debate in the field of experimental psychology [Dixon, 1971] and more recently in cognitive neuroscience [Dehaene and Changeux, 2011; Kouider and Dehaene, 2007]. Over the years, and in parallel with the development of modern neuroimaging methods, a great emphasis has been put on studying nonconscious perception using primarily emotional or meaningful stimuli in combination with visual masking paradigms [Tamietto and de Gelder, 2010; Wiens, 2006]. Here, we studied the EEG brain responses in human participants to subliminally presented unmasked visual stimuli using a highly chronometrically precise LCD tachistoscope [Sperdin et al., 2013].

First, we performed a TCT to identify whether the checkerboard (Experiment 1) and/or the white stimulus (Experiment 2) consistently evoked a brain response [Koenig et al., 2011; Koenig and Melie-Garcia, 2009; Koenig and Melie-Garcia, 2010]. That is, we tested for the presence of a signal in the multichannel ERP data (as opposed to noise). As a consistent topography at a certain latency across participants is one of the defining attributes of an evoked potential component [De Lucia et al., 2010; Spencer et al., 2001] finding evidence for the presence of consistent topographies would indicate that the measured activity does not only represent noise, but a consistent brain response functionally related to the repeated presentation of stimuli. In Experiment 1, the TCT revealed the presence of periods of sustained and consistent topographies in response to the repeated presentation of the checkerboards for 1 ms, for 500 μs and even for the extreme short duration of 250 μs. In the latter condition, the screen was perceived as remaining white throughout the recording blocks of interest as was verbally reported by the participants, and as was confirmed by the results of the forced-choice detection task (Experiment 3). This indicates no conscious awareness of the visual stimulus [Naccache and Dehaene, 2001; Snodgrass et al., 2004]. Conversely, the white stimulus condition (Experiment 2) did not evoke any sustained periods of consistent topographies, indicating that the stimulus did not evoke any electrical brain response.

Mean onset latency of the initial activity in the visual cortex has been shown to vary from 25 to around 100 ms using VEPs/VEFs and to differ with respect to the type of stimuli, and measurements used [Cobb and Dawson, 1960; Di Russo et al., 2002; Foxe and Simpson, 2002; Inui and Kakigi, 2006; Inui et al., 2006; Moradi et al., 2003; Portin et al., 1999; Yesilyurt et al., 2010; Yoneda et al., 1995]. Here, the TCT revealed in Experiment 1 a brain response to the stimuli from 24 ms post-stimulus onset onward in the 1 ms condition and at 16 ms post-stimulus onset onward for the 250 μs condition. Those onsets are rather early compared to the known conduction delays usually reported by human and animal experiments. Only the 500 μs condition indicated an onset of stable topographies at usually reported latency (56 ms). For the TCT performed on the data of Experiment 2 where the checkerboards was replaced by a blank control stimulus, the test also revealed early short lived periods of stable topographies that are more likely noise related because of the early latencies at which they occurred (at −35 ms for the 1 ms condition, 5 ms for the 500 μs condition and 24 ms for the 250 μs

condition). When looking on the other hand at the time-wise statistical contrasts of mean GFP waveforms, it becomes evident that the brain started to respond more strongly to the checkerboard at 63 ms post-stimulus onset for the 1 ms condition at 74 ms post-stimulus onset for the 500 μs condition and at 83 ms post-stimulus onset for the 250 μs condition, latencies more in line with those previously reported in the literature cited above.

Many VEP components have been proposed as possible correlates of visual consciousness in experiments contrasting seen versus unseen visual stimuli [Dehaene and Changeux, 2011, for recent reviews; Koivisto and Revonsuo, 2010]. Some studies have identified amplitude and or/latency shifts during the first positive-going component at 100 ms post-stimulus onset (P1) when manipulating the contrast [Aru and Bachmann, 2009; Pins and Ffytche, 2003; Wilenius and Revonsuo, 2007] or by masking the target stimuli [Del Cul et al., 2007]. Modulations during the first and second negative-going VEP components (N1-N2) have also been proposed as signatures of visual consciousness [Del Cul et al., 2007; Genetti et al., 2009; Koivisto et al., 2009; Melloni et al., 2011; Railo and Koivisto, 2009; Wilenius-Emet et al., 2004] followed by an enhanced late positivity in the P3 range starting around 300 ms post stimulus onset or even later [Aru and Bachmann, 2009; Babiloni et al., 2006; Dehaene et al., 2001; Del Cul et al., 2007; Genetti et al., 2009; Lamy et al., 2009; Sergent et al., 2005]. However, drawing unequivocal conclusions on which EEG component reflects true neural markers of perceptual consciousness still remains debated and difficult to address with respect to the divergences and variety of experimental designs, stimuli, tasks, and different measures used [Dehaene and Changeux, 2011; Kim and Blake, 2005; Koivisto and Revonsuo, 2010; Lamme, 2006; Overgaard and Sandberg, 2012; Sandberg et al., 2010].

In the case of EEG studies of subliminal perception, the evoked responses of a target subliminal stimulus in masked paradigms are inevitably contaminated by the mask because they overlap in time [Enns and Di Lollo, 2000; Fahrenfort et al., 2007; Lamme et al., 2002]. Even if a few experiments have tried to elucidate the effect of the mask on a given electrophysiological signal [e.g., Andreassi et al., 1976; Kovacs et al., 1995; Lamme et al., 2002; Schiller and Chorover, 1966], here we circumvented the methodological limitation by simply not using a mask.

Subliminal perception has been studied with exposure durations ranging from 1 to 20 milliseconds using cumbersome mechanical or electrical tachistoscopes (Bernat et al., 2001; Henke et al., 1994; Kostandov and Arzumanov, 1977; Kunstwilson and Zajonc, 1980; Landis et al., 1992; Shevrin, 2001; Shevrin and Fritzler, 1968] but never at shorter submillisecond exposures, nor in combination with modern neuroimaging methods. Moreover, older mechanical and electrical tachistoscopes have been largely criticized because of their lack of reliability, principally because of the components they were made of or the variability of the chronometrical measures [e.g., Bohlander, 1979; Glaser, 1988; Madigan and Johnson, 1991; Merikle, 1980; Mollon and Polden, 1978]. Here, we presented the stimuli using a highly reliable LCD tachistoscope having a precision of 3 μs, enabling to determine accurately what stimulus was available for the visual system and for how long.

We found that the brain responses to the presented checkerboards modulated topographically as function of the exposure duration between 243 and 296 ms post-stimulus onset indicating the engagement of distinct configurations of intracranial generators over that specific time period [Fender, 1987; Murray et al., 2008]. Source estimation localized this effect in the right parietal cortex, within BA 7/19 and with a maximum around the right precuneus. This region is known to play a central role in conscious information processing [Cavanna, 2007; Vogt and Laureys, 2005 for review]. For example, modulation of activity in this area has been shown using masked words [Kjaer et al., 2001]. In this PET experiment, the authors found that words that transitioned from a subliminal stage (that is, they could not be detected) to a more liminal one (that is, they entered consciousness) was correlated with an increase of activity within that region, suggesting a critical role played for visual consciousness. Our behavioral results would support a similar interpretation: the transition from a completely unseen subliminal visual meaningless stimulus (in the 250 μs condition) toward a more liminal stage (1 ms) modulates activity within this cortical locus. In general, agreement with this interpretation are findings of numerous studies highlighting posterior parietal cortical regions as part of a larger brain network encompassing temporo-frontal nodes associated with perceptual consciousness [Babiloni et al., 2006; Dehaene and Changeux, 2011, for recent review; Dehaene et al., 2001; Del Cul et al., 2007].

In conclusion, our results are a proof of concept of our LCD tachistoscope as it shows that it is possible to study subliminal stimulation without using masking in combination with modern electrical neuroimaging analysis methods. These results further show the presence of a brain response to submillisecond unmasked subliminal visual stimuli independently of their emotional saliency or meaningfulness.

ACKNOWLEDGMENTS

Cartool software (http://sites.google.com/site/fbmlab/cartool) has been programmed by Denis Brunet, from the Functional Brain Mapping Laboratory, Geneva, Switzerland, supported by the Lemanic Biomedical Imaging Center (CIBM). The STEN toolbox http://www.unil.ch/fenl/home/menuinst/about-the-line/software–analysis-tools.html) has been programmed by Jean-François Knebel, from the Laboratory for Investigative Neurophysiology (the LINE), Lausanne, Switzerland, and supported by the Lemanic Biomedical Imaging Center (CIBM). We thank Marc Repnow and Christophe Mermoud for technical assistance. We thank the anonymous reviewers for their helpful comments on earlier versions of this manuscript.

REFERENCES

Andreassi JL, De Simone JJ, Mellers BW (1976): Amplitude changes in the visual evoked cortical potential with backward masking. Electroencephalogr Clin Neurophysiol 41:387–398.

Aru J, Bachmann T (2009): Occipital EEG correlates of conscious awareness when subjective target shine-through and effective visual masking are compared: Bifocal early increase in gamma power and speed-up of P1. Brain Res 1271:60–73.

Babiloni C, Vecchio F, Miriello M, Romani GL, Rossini PM (2006): Visuo-spatial consciousness and parieto-occipital areas: A high-resolution EEG study. Cereb Cortex 16:37–46.

Bernat E, Bunce S, Shevrin H (2001): Event-related brain potentials differentiate positive and negative mood adjectives during both supraliminal and subliminal visual processing. Int J Psychophysiol 42:11–34.

Bohlander RW (1979): Luminance of Tachistoscope Lamps as a Function of Flash Duration. Behav Res Methods Instrum 11: 414–418.

Brainard DH (1997): The Psychophysics Toolbox. Spat Vis 10:433–436.

Brunet D, Murray MM, Michel CM (2011): Spatiotemporal analysis of multichannel EEG: CARTOOL. Comput Intell Neurosci 2011:813870.

Bukhari F, Kurylo DD (2008): Computer programming for generating visual stimuli. Behav Res Methods 40:38–45.

Cavanna AE (2007): The precuneus and consciousness. CNS Spectr 12:545–552.

Cobb, W.A., Dawson, G.D. (1960): The latency and form in man of the occipital potentials evoked by bright flashes. J Physiol 152:108–121.

De Lucia M, Michel CM, Murray MM (2010): Comparing ICA-based and single-trial topographic ERP analyses. Brain Topogr 23:119–127.

Dehaene S, Changeux JP (2011): Experimental and theoretical approaches to conscious processing. Neuron 70:200–227.

Dehaene S, Naccache L, Cohen L, Bihan DL, Mangin JF, Poline JB, Riviere D (2001): Cerebral mechanisms of word masking and unconscious repetition priming. Nat Neurosci 4:752–758.

Del Cul A, Baillet S, Dehaene S (2007): Brain dynamics underlying the nonlinear threshold for access to consciousness. PLoS Biol 5:e260.

Di Russo F, Martinez A, Sereno MI, Pitzalis S, Hillyard SA (2002): Cortical sources of the early components of the visual evoked potential. Hum Brain Mapp 15:95–111.

Dixon NF (1971): Subliminal Perception: The Nature of a Controversy. London. McGraw-Hill.

Efron R (1964): Artificial synthesis of evoked responses to light flash. Ann N Y Acad Sci 112:292–304.

Enns JT, Di Lollo V (2000): What's new in visual masking? Trends Cogn Sci 4:345–352.

Fahrenfort JJ, Scholte HS, Lamme VA (2007): Masking disrupts reentrant processing in human visual cortex. J Cogn Neurosci 19:1488–1497.

Fender DH (1987): Source localisation of brain electrical activity. In: Gevins AS, Remond A, editors. Handbook of Electroencephalography and Clinical Neurophysiology, Vol. 1: Methods of Analysis of Brain Electrical and Magnetic Signals. Amsterdam: Elsevier. pp 355–399.

Foxe JJ, Simpson GV (2002): Flow of activation from V1 to frontal cortex in humans. A framework for defining "early" visual processing. Exp Brain Res 142:139–150.

Genetti M, Khateb A, Heinzer S, Michel CM, Pegna AJ (2009): Temporal dynamics of awareness for facial identity revealed with ERP. Brain Cogn 69:296–305.

Glaser WR (1988): Technical Improvements to the Projection Tachistoscope. Behav Res Meth Instrum 20:491–494.

Grave de Peralta Menendez R, Gonzalez Andino S, Lantz G, Michel CM, Landis T (2001): Noninvasive localization of electromagnetic epileptic activity. I. Method descriptions and simulations. Brain Topogr 14:131–137.

Grave de Peralta Menendez R, Murray MM, Michel CM, Martuzzi R, Gonzalez Andino SL (2004): Electrical neuroimaging based on biophysical constraints. Neuroimage 21:527–539.

Green DM, Swets JA (1988): Signal detection theory and psychophysics. Los Altos, California: Peninsula Publishing. xiii, 505 p.

Griffing H (1896): On the development of visual perception and attention. Ame J Psychol 7:227–236.

Guthrie D, Buchwald JS (1991): Significance testing of difference potentials. Psychophysiology 28:240–244.

Henke K, Landis T, Markowitsch HJ (1994): Subliminal perception of words and faces. Int J Neurosci 75:181–187.

Inui K, Kakigi R (2006): Temporal analysis of the flow from V1 to the extrastriate cortex in humans. J Neurophysiol 96:775–784.

Inui K, Sannan H, Miki K, Kaneoke Y, Kakigi R (2006): Timing of early activity in the visual cortex as revealed by simultaneous MEG and ERG recordings. Neuroimage 30:239–244.

Karlin L (1955): The New York University tachistoscope. Am J Psychol 68:462–466.

Karremans JC, Stroebe W, Claus J (2006): Beyond Vicary's fantasies: The impact of subliminal priming and brand choice. J Exp Soc Psychol 42:792–798.

Kim CY, Blake R (2005): Psychophysical magic: Rendering the visible 'invisible'. Trends Cogn Sci 9:381–358.

Kjaer TW, Nowak M, Kjaer KW, Lou AR, Lou HC (2001): Precuneus-prefrontal activity during awareness of visual verbal stimuli. Conscious Cogn 10:356–365.

Koenig T, Melie-Garcia L (2009): Statistical analysis of multichannel scalp field data. In: Michel CM, Koenig T, Brandeis D, Gianotti LR, Wackermann J, editors. Electrical neuroimaging. Cambridge University Press: Cambridge University Press.

Koenig T, Melie-Garcia L (2010): A method to determine the presence of averaged event-related fields using randomization tests. Brain Topogr 23:233–242.

Koenig T, Kottlow M, Stein M, Melie-Garcia L (2011): Ragu: A free tool for the analysis of EEG and MEG event-related scalp field data using global randomization statistics. Comput Intell Neurosci 2011:938925.

Koenig T, Stein M, Grieder M, Kottlow M (2013): A tutorial on data-driven methods for statistically assessing ERP topographies. Brain Topogr 27:72–83.

Koivisto M, Revonsuo A (2010): Event-related brain potential correlates of visual awareness. Neurosci Biobehav Rev 34:922–934.

Koivisto M, Kainulainen P, Revonsuo A (2009): The relationship between awareness and attention: Evidence from ERP responses. Neuropsychologia 47:2891–2899.

Kostandov E, Arzumanov Y (1977): Averaged cortical evoked potentials to recognized and non-recognized verbal stimuli. Acta Neurobiol Exp 37:311–324.

Kouider S, Dehaene S (2007): Levels of processing during non-conscious perception: A critical review of visual masking. Philos Trans R Soc Lond Ser B Biol Sci 362:857–875.

Kouider S, Stahlhut C, Gelskov SV, Barbosa LS, Dutat M, de Gardelle V, Christophe A, Dehaene S, Dehaene-Lambertz G

(2013): A neural marker of perceptual consciousness in infants. Science 340:376–380.
Kovacs G, Vogels R, Orban GA (1995): Cortical correlate of pattern backward masking. Proc Natl Acad Sci USA 92:5587–5591.
Krantz JH (2000): Tell me, what did you see? The stimulus on computers. Behav Res Methods Instrum Comput 32:221–229.
Kunstwilson WR, Zajonc RB (1980): Affective discrimination of stimuli that cannot be recognized. Science 207:557–558.
Lamme VA (2006): Towards a true neural stance on consciousness. Trends Cogn Sci 10:494–501.
Lamme VA, Zipser K, Spekreijse H (2002): Masking interrupts figure-ground signals in V1. J Cogn Neurosci 14:1044–1053.
Lamy D, Salti M, Bar-Haim Y (2009): Neural correlates of subjective awareness and unconscious processing: An ERP study. J Cogn Neurosci 21:1435–1446.
Lancaste GA, Sayer I, Scott AE, Sutcliff RM (1971): Development and use of mechanical tachistoscope. Eur J Marketing 5:30–35.
Landis T, Christen L, Graves R (1992): Dissociated hemispheric and stimulus effects upon affective choice and recognition. Int J Neurosci 62:81–87.
Lehmann D, Skrandies W (1980): Reference-free identification of components of checkerboard-evoked multichannel potential fields. Electroencephalogr Clin Neurophysiol 48:609–621.
Macmillan NA, Creelman CD (2005): Detection Theory: A User's Guide. New York, London: Psychology Press. xix, 492 p.
Madigan R, Johnson S (1991): Measuring projection tachistoscope shutter characteristics. Behav Res Methods Instrum 23:23–26.
Melloni L, Schwiedrzik CM, Muller N, Rodriguez E, Singer W (2011): Expectations change the signatures and timing of electrophysiological correlates of perceptual awareness. J Neurosci 31:1386–1396.
Merikle PM (1980): Selective masking and the lamp-phosphor problem. Q J Exp Psychol 32:491–495.
Merryman JG, Allen HE (1953): An improved electronic tachistoscope. Am J Psychol 66:110–114.
Michel CM (2009): Electrical neuroimaging. Cambridge, New York. Cambridge University Press. x, 238 p.
Michel CM, Murray MM (2012): Towards the utilization of EEG as a brain imaging tool. Neuroimage 61:371–385.
Michel CM, Murray MM, Lantz G, Gonzalez S, Spinelli L, Grave de Peralta R (2004): EEG source imaging. Clin Neurophysiol 115:2195–2222.
Mollon JD, Polden PG (1978): Time constants of tachistoscopes. Q J Exp Psychol 30:555–568.
Moradi F, Liu LC, Cheng K, Waggoner RA, Tanaka K, Ioannides AA (2003): Consistent and precise localization of brain activity in human primary visual cortex by MEG and fMRI. Neuroimage 18:595–609.
Murray MM, Brunet D, Michel CM (2008): Topographic ERP analyses: A step-by-step tutorial review. Brain Topogr 20:249–264.
Naccache L, Dehaene S (2001): Unconscious semantic priming extends to novel unseen stimuli. Cognition 80:215–229.
Nichols TE, Holmes AP (2002): Nonparametric permutation tests for functional neuroimaging: A primer with examples. Hum Brain Mapp 15:1–25.
Oldfield RC (1971): The assessment and analysis of handedness: The Edinburgh inventory. Neuropsychologia 9:97–113.
Overgaard M, Sandberg K (2012): Kinds of access: Different methods for report reveal different kinds of metacognitive access. Philos Trans R Soc Lond B Biol Sci 367:1287–1296.
Peirce JW (2007): PsychoPy—Psychophysics software in Python. J Neurosci Methods 162:8–13.
Perrin F, Pernier J, Bertrand O, Giard MH, Echallier JF (1987): Mapping of scalp potentials by surface spline interpolation. Electroencephalogr Clin Neurophysiol 66:75–81.
Pins D, Ffytche D (2003): The neural correlates of conscious vision. Cereb Cortex 13:461–474.
Portin K, Vanni S, Virsu V, Hari R (1999): Stronger occipital cortical activation to lower than upper visual field stimuli. Neuromagnetic recordings. Exp Brain Res 124:287–294.
Railo H, Koivisto M (2009): The electrophysiological correlates of stimulus visibility and metacontrast masking. Conscious Cogn 18:794–803.
Sandberg K, Timmermans B, Overgaard M, Cleeremans A (2010): Measuring consciousness: Is one measure better than the other? Conscious Cogn 19:1069–1078.
Schiller PH, Chorover SL (1966): Metacontrast: Its relation to evoked potentials. Science 153:1398–1400.
Sergent C, Baillet S, Dehaene S (2005): Timing of the brain events underlying access to consciousness during the attentional blink. Nat Neurosci 8:1391–1400.
Shevrin H (2001): Event-related markers of unconscious processes. Int J Psychophysiol 42:209–218.
Shevrin H, Fritzler DE (1968): Visual evoked response correlates of unconscious mental processes. Science 161:295–298.
Snodgrass M, Bernat E, Shevrin H (2004): Unconscious perception: A model-based approach to method and evidence. Percept Psychophys 66:846–867.
Spencer KM, Dien J, Donchin E (2001): Spatiotemporal analysis of the late ERP responses to deviant stimuli. Psychophysiology 38:343–358.
Sperdin HF, Repnow M, Herzog MH, Landis T (2013): An LCD tachistoscope with submillisecond precision. Behav Res Methods 45:1345–1357.
Talairach J, Tournoux P (1988): Co-Planar Stereotaxic Atlas of the Human Brain: 3-Dimensional Proportional System: An Approach to Cerebral Imaging. Stuttgart, New York: Georg Thieme. 122 p.
Tamietto M, de Gelder B (2010): Neural bases of the non-conscious perception of emotional signals. Nat Rev Neurosci 11:697–709.
Vogt BA, Laureys S (2005): Posterior cingulate, precuneal and retrosplenial cortices: Cytology and components of the neural network correlates of consciousness. Prog Brain Res 150:205–217.
Wiens S (2006): Current concerns in visual masking. Emotion 6: 675–680.
Wiens S, Fransson P, Dietrich T, Lohmann P, Ingvar M, Öhman A (2004): Keeping it short: A comparison of methods for brief picture presentation. Psychol Sci 15:282–285.
Wiens S, Öhman A (2005): Visual masking in magnetic resonance imaging. Neuroimage 27:465–467.
Wilenius-Emet M, Revonsuo A, Ojanen V (2004): An electrophysiological correlate of human visual awareness. Neurosci Lett 354:38–41.
Wilenius ME, Revonsuo AT (2007): Timing of the earliest ERP correlate of visual awareness. Psychophysiology 44:703–710.
Yesilyurt B, Whittingstall K, Ugurbil K, Logothetis NK, Uludag K (2010): Relationship of the BOLD signal with VEP for ultrashort duration visual stimuli (0.1 to 5 ms) in humans. J Cereb Blood Flow Metab 30:449–458.
Yoneda K, Sekimoto S, Yumoto M, Sugishita M (1995): The early component of the visual evoked magnetic field. Neuroreport 6: 797–800.